Crystal Structures and Magnetic Properties of $NaK_3(NpO_2)_4(SO_4)_4(H_2O)_2$ and $NaNpO_2SO_4H_2O$: Cation−Cation Interactions in a Neptunyl Sulfate Framework

Tori Z. Forbes,[†] Peter. C. Burns,*[,†,‡] L. Soderholm,[†,‡] and S. Skanthakumar[‡]

Department of Civil Engineering and Geological Sciences, University of Notre Dame, 156 Fitzpatrick Hall, Notre Dame, Indiana 46556, and Chemistry Division, Argonne National Laboratory, Argonne, Illinois 60439

Received October 27, 2005. Revised Manuscript Received January 20, 2006

Two novel neptunium(V) sulfates, $NaK_3(NpO_2)_4(SO_4)_4(H_2O)_2$ and $NaNpO_2SO_4H_2O$, have been prepared by hydrothermal methods. The structure of each has been determined by single-crystal X-ray diffraction using Mo Kα radiation and a charge-coupled device area detector. Both structures are monoclinic with space group *C*2/*c*. $NaK_3(NpO_2)_4(SO_4)_4(H_2O)_2$ ($R_1 = 0.0351$) has unit cell parameters $a = 18.0998(12)$, $b = 5.7030(4)$, $c = 23.1988(16)$, $\beta = 104.6330(10)°$, $V = 2317.0(3)$ Å^3, and $Z = 16$. $NaNpO_2SO_4H_2O$ ($R_1 = 0.036$) has unit cell parameters $a = 18.3638(13)$, $b = 5.6424(4)$, $c = 23.5512(17)$, $\beta = 103.366(2)°$, $V = 2374.2(3)$ Å^3, and $Z = 16$. Both structures contain chains of $Np(V)O_7$ pentagonal bipyramids linked into a framework structure through the sulfate tetrahedra. The neptunyl polyhedra are involved in multiple cation−cation interactions. Magnetic susceptibility data, together with field-dependent studies, indicate the presence of ferromagnetic ordering at 6.5(5) K for $NaK_3(NpO_2)_4(SO_4)_4(H_2O)_2$ and 7.4(1) K for $NaNpO_2SO_4H_2O$.

Introduction

^{237}Np ($t_{1/2} = 2.14 \times 10^6$ years) is a man-made element that is considered to be one of the most problematic radionuclides for nuclear-waste storage in a long-term geologic repository.[1] Initially ^{237}Np is produced as a byproduct in nuclear reactors, but because of radioactive decay of ^{241}Am ($t_{1/2} = 432.7$ years) the concentration of ^{237}Np increases in spent fuel through the first several thousand years. It is expected to be a major dose contributor in a geologic repository such as Yucca Mountain.[1] Understanding the basics of the structural chemistry of neptunium is vital for addressing its geochemical behavior and risk assessment of nuclear waste disposal.[1−3] Unfortunately there are very few published crystal structures that contain neptunium in its most environmentally important predominant oxidation state, Np^{5+}.

As ^{237}Np is not a naturally occurring element, there are no geological natural analogues for developing an understanding of the crystal structures and chemical behavior of Np^{5+}. As a result of the scarcity of structural data for neptunium compounds, it is tempting to proclaim that the structural chemistry of Np^{5+} will mirror that of U^{6+}. Substantial progress has been made in advancing understanding of the crystal chemistry of U^{6+}, and the structures are known for approximately 370 inorganic structures that contain essential uranyl, of which 89 are minerals.[4]

Both uranium and neptunium are redox-sensitive radionuclides, which makes their chemical behavior qualitatively similar.[5,6] Uranium occurs in nature in both the tetravalent and the hexavalent states; however, only the hexavalent state is significantly soluble, and it forms the dioxo $(UO_2)^{2+}$ cation.[7] In contrast, neptunium has four common oxidation states, III, IV, V, and VI, with pentavalent neptunium, present as a linear dioxo cation, $[O{=}Np{=}O]^+$, the most stable moiety in solution.[1,5]

Actinide (VI) compounds such as uranium almost invariably contain approximately linear $(AnO_2)^{2+}$ dioxide cations that are further coordinated by four, five, or six ligands, giving square, pentagonal, or hexagonal bipyramids.[8−10] In the case of the $(AnO_2)^{2+}$ cation, the bonding requirements of the O atoms are nearly met by the bond to the An^{6+} cation alone, and these O atoms seldom bond to other cations of higher valence.[3] Relatively little is known about the crystal chemistry of actinide (V) compounds, but of the structures reported, a significant fraction contain a linear $(AnO_2)^+$ dioxide cation similar in geometry to those found for the hexavalent state. However, the lower charge of the An^{5+} cation in $(AnO_2)^+$ results in somewhat weaker bonds to the O atoms in the dioxide cation, relative to the bonds in $(AnO_2)^{2+}$ cations. In other words, the O atoms of the $(AnO_2)^+$

* Corresponding author. Fax: 574-631-9236. E-mail address: pburns@nd.edu.
† University of Notre Dame.
‡ Argonne National Laboratory.

(1) Kaszuba, J. P.; Runde, W. H. *Environ. Sci. Technol.* **1999**, *33*, 4427−4433.
(2) Lieser, K. H.; Muhlenweg, U. *Radiochim. Acta* **1988**, *43*, 27−35.
(3) Burns, P. C.; Ewing, R. C.; Hawthorne, F. C. *Can. Mineral.* **1997**, *35*, 1551−1570.
(4) Burns, P. C. *Can. Mineral.* **2005**, *43*, 1839−1894.
(5) Antonio, M. R.; Soderholm, L.; Williams, C. C.; Blaudeau, J.-P.; Bursten, B. E. *Radiochim. Acta* **2001**, *89*, 17−25.
(6) Silva, R. J.; Nitsche, H. *Radiochim. Acta* **1995**, *70/71*, 377−396.
(7) Aspinall, H. C. *Chemistry of the f Block Elements*; Gordon and Breach Science Publishers: Singapore, 2001; p 154.
(8) Evans, H. T. J. *Science* **1963**, *141*, 154−157.
(9) Weigel, F. *Uranium*, 2nd ed.; Chapman and Hall: London, 1986.
(10) Burns, P. C.; Miller, M. L.; Ewing, R. C. *Can. Mineral.* **1996**, *34*, 845−880.

10.1021/cm0523687 CCC: $33.50
Published on Web 02/25/2006

ion will tend to form bonds with other cations somewhat stronger than those in $(AnO_2)^{2+}$. Thus, the crystal chemistries of pentavalent and hexavalent actinides may diverge to meet the bonding requirements of the O atoms of the $(AnO_2)^{+}$ cation. We hypothesize that $(Np(VI)O_2)^{2+}$ can be expected to largely follow the structural trends of $(U(VI)O_2)^{2+}$ but that $(Np(V)O_2)^{+}$ will crystallize with new structure types that are able to accommodate the bonding requirements of the O atoms.

The bonding requirements of the O atoms of the $(Np(V)O_2)^{+}$ cation may be met through interactions with other $(Np(V)O_2)^{+}$ cations. Specifically, an O atom of one linear $[O{=}Np{=}O]^{+}$ ion can also coordinate as the equatorial ligand of a neighboring $(Np(V)O_2)^{+}$ polyhedron. First postulated from solution studies,[12] the direct linkage of two actinyl ions through the bonding of an oxo ion from one $(AnO_2)^{+}$ moiety as the equatorial ligand on an adjacent $(AnO_2)^{+}$ ion has been designated as a cation−cation interaction. Such interactions are relatively common in the reported structures that contain Np^{5+} [11] but are much more unusual in the case of U^{6+}.[13] Linkage of uranyl bipyramids with other polyhedra is almost invariably through the equatorial vertexes of the bipyramids.[10] The potential for cation−cation interactions in Np^{5+} structures suggests significant divergence from U^{6+}crystal chemistry and structural connectivities.

We are undertaking a detailed study of Np^{5+} crystal chemistry, focusing on compounds with environmentally relevant chemical compositions, to develop better insight into Np^{5+} crystal chemistry and to provide a basis for furthering the fundamental understanding of Np^{5+} solution chemistry. Here we report the structures of two isostructural Np^{5+} sulfates that possess a novel framework of polyhedra that includes cation−cation interactions. We also report the magnetic properties of these compounds and comment on their unusual behavior with respect to their structural connectivity.

Experimental Section

Crystal Synthesis. The reagents K_2SO_4 (Fisher Scientific lot no. 783390), $Na_2SO_4(H_2O)_{10}$ (Baker lot no. 28106), NaOH (Fisher Scientific lot no. 975017), and KOH (Fisher Scientific lot no. 876491) were used as received. A Np^{5+} stock solution was prepared in a 1 M HCl solution. *Caution: ^{237}Np represents a serious health risk due to the emission of alpha and gamma radiation. All studies were conducted in the actinide facilities of Argonne National Laboratory, which has appropriate equipment and personnel for handling such materials.* All reactions took place in 7 mL Teflon cups with screw-top lids. After loading the reactants, the tightly closed Teflon cups were placed in 125 mL Teflon lined Parr acid reaction vessels. Fifty milliliters of ultrapure water (18 MΩ resistance) was added to each vessel to provide counterpressure during heating.

$NaK_3(NpO_2)_4(SO_4)_4(H_2O)_2$ (KS2-2) was synthesized by the hydrothermal reaction of 0.0441 g of K_2SO_4 with 0.45 mL of a 0.109 M Np^{5+} solution (11.26 mg of Np) and 0.55 mL of ultrapure water (final concentration of Np in solution was 0.050 M). The pH was adjusted from 0.79 to 1.95 by addition of 52 μL of 5 M KOH. The mixture was heated for 1 week at 150 °C in a gravity convection oven and was allowed to cool slowly in the oven. Dark green platy crystals ~600 μm in length were obtained. The structure determination indicated the presence of a Na cation in the KS2-2 structure, and this was verified by energy dispersive spectrometry using a LEO EVO-50XVP variable pressure/high humidity scanning electron microscope. The Na was an impurity in the Np stock solution.

Table 1. Crystal Data and Structure Refinement for KS2-2 and NaS2-2

	KS2-2	NaS2-2
structure formula	$NaK_3(NpO_2)_4(SO_4)_4(H_2O)_2$	$NaNpO_2SO_4H_2O$
formula weight	1604.53	406.06
temperature (K)	293(2)	293(2)
wavelength (Å)	0.710 73	0.710 73
space group	*C*2/*c* (No. 15)	*C*2/*c* (No. 15)
a (Å)	18.0998(12)	18.3638(13)
b (Å)	5.7030(4)	5.6424(4)
c (Å)	23.1988(16)	23.5512(17)
β (deg)	104.633(1)	103.366(2)
volume (Å^3)	2317.0(3)	2374.2(3)
Z	16	16
density (g/cm^3)	4.692	4.544
μ (mm^{-1})	18.986	17.911
F(000)	2864	2848
crystal size (mm)	0.100 × 0.080 × 0.040	0.075 × 0.050 × 0.010
theta range for data collection (deg)	2.33−34.56	2.28−34.50
limiting indices	$-28 < h < 28$, $-9 < k < 8$, $-36 < l < 36$	$-28 < h < 28$, $-5 < k < 8$, $-36 < l < 36$
reflections collected/ unique	22 579/4842 [$R_{int} = 0.0700$]	11 701/4817 [$R_{int} = 0.0416$]
refinement method	full-matrix least-squares on F^2	full-matrix least-squares on F^2
data/restraints/ parameters	4842/2/180	4817/4/197
goodness-of-fit on F^2	1.073	0.967
final *R* indices [$I > 2\sigma(I)$]	R1 = 0.0351, wR2 = 0.0717	R1 = 0.0363, wR2 = 0.0596
R indices (all data)	R1 = 0.0405, wR2 = 0.0736	R1 = 0.0623, wR2 = 0.0667
largest diff. peak and hole (Å^3)	4.248 and −2.777	2.155 and −2.228

$Na(NpO_2)(SO_4)(H_2O)$ (NaS2-2) was synthesized by hydrothermal reaction of 0.0817 g of $Na_2SO_4(H_2O)_{10}$ with 0.64 mL of 0.078 M Np^{5+} stock solution (11.83 mg Np) and 0.36 mL of ultrapure water (final concentration of Np was 0.05 M). The pH was adjusted from 0.48 to 2.01 by addition of 64 μL of a 5 M NaOH solution. The reaction vessel was heated at 150 °C for 1 week and was then allowed to cool slowly to room temperature in the oven. Dark green crystals ~600 μm in length formed during the reaction.

Single-Crystal X-ray Diffraction. A suitable single crystal of each compound was selected and mounted on a glass fiber for the X-ray study. Single-crystal X-ray diffraction data were collected using a Bruker PLATFORM three-circle X-ray diffractometer equipped with a 4 K APEX charge-coupled device detector. A sphere of three-dimensional data was collected for KS2-2 at room temperature using monochromatic Mo Kα radiation, frame widths of 0.3° in ω, and 30 s spent counting per frame. A hemisphere of data was collected for NaS2-2 using frame widths of 0.3° in ω and a count time of 120 s per frame. Unit cell parameters were refined by least-squares techniques using the Bruker SMART software.[14] Selected data collection parameters and crystallographic data are provided in Table 1.

Data for each crystal were integrated and corrected for Lorentz, polarization, and background effects using the Bruker program

(11) Krot, N. N.; Grigoriev, M. S. *Russ. Chem. Rev.* **2004**, *73*, 89−100.
(12) Sullivan, J. C.; Hindman, J. C.; Zielen, A. J. *J. Am. Chem. Soc.* **1961**, *83*, 3373−3378.
(13) Sullens, T. A.; Jensen, R. A.; Shvareva, T. Y.; Albrecht-Schmitt, T. E. *J. Am. Chem. Soc.* **2004**, *126*, 2676−2677.
(14) *SHELXTL Programs*, version 5.01; Bruker Analytical X-ray Systems: Madison, WI, 1998.

Table 2. Selected Bond Lengths [Å] for KS2-2

Np(1)−O(7)[a]	1.827(4)	Na(1)−O(11)	2.409(4)
Np(1)−O(9)	1.856(4)	Na(1)−O(11)[g]	2.410(4)
Np(1)−O(2)[a]	2.404(4)	Na(1)−O(7)	2.493(4)
Np(1)−O(6)[a]	2.453(4)	Na(1)−O(7)[g]	2.493(4)
Np(1)−O(3)	2.469(4)	Na(1)−O(1)[h]	2.550(4)
Np(1)−O(1)	2.487(4)	Na(1)−O(1)[i]	2.551(4)
Np(1)−O(8)	2.494(4)	Na(1)−O(3)	2.831(4)
		Na(1)−O(3)[g]	2.831(4)
Np(2)−O(6)	1.828(4)		
Np(2)−O(10)	1.852(4)	S(1)−O(13)	1.458(4)
Np(2)−O(11)	2.431(4)	S(1)−O(12)[a]	1.466(4)
Np(2)−O(9)	2.443(4)	S(1)−O(2)[c]	1.484(4)
Np(2)−O(4)	2.453(4)	S(1)−O(8)	1.488(4)
Np(2)−O(10)[b]	2.462(4)		
Np(2)−O(5)	2.535(4)	S(2)−O(4)[j]	1.469(4)
		S(2)−O(3)[g]	1.470(4)
K(1)−O(2)[c]	2.658(4)	S(2)−O(1)	1.473(4)
K(1)−O(2)	2.658(4)	S(2)−O(11)	1.484(4)
K(1)−O(12)[c]	2.723(4)		
K(1)−O(12)	2.723(4)		
K(1)−O(8)	2.832(4)		
K(1)−O(8)[c]	2.832(4)		
K(1)−O(9)[c]	3.227(4)		
K(1)−O(9)	3.227(4)		
K(2)−O(12)	2.756(5)		
K(2)−O(13)[d]	2.835(5)		
K(2)−O(7)	2.915(4)		
K(2)−O(4)[e]	2.942(4)		
K(2)−O(8)	2.981(4)		
K(2)−O(5)[f]	2.992(5)		
K(2)−O(3)	3.008(4)		

[a −j]Symmetry transformations used to generate equivalent atoms: (a) $x, y + 1, z$; (b) $-x + 1/2, y + 1/2, -z + 1/2$; (c) $-x, -y + 1, -z$; (d) $-x - 1/2, -y + 3/2, -z$; (e) $x - 1/2, y + 1/2, z$; (f) $x - 1/2, y - 1/2, z$; (g) $-x, y, -z + 1/2, z$; (h) $x, y - 1, z$; (i) $-x, y - 1, -z + 1/2$; (j) $x + 1/2, y - 1/2, z$.

SAINT.[14] Semi-empirical corrections for absorption were applied by modeling the crystals as ellipsoids using the Bruker program XPREP, which lowered R_{INT} from 0.127 to 0.070 for KS2-2 and from 0.054 to 0.027 for NaS2-2.[14] KS2-2 and NaS2-2 are isostructural and systematic absences of reflections indicated by space groups *Cc* or *C*2/*c*. In both cases *C*2/*c* was verified by successful solution and refinement of the structure using the SHELXTL, version 5, programs. Np, K, and Na positions were determined using direct methods, and S and O positions were located in difference Fourier maps calculated following subsequent refinement cycles. Possible H atom positions consistent with estimated bond lengths were located in the difference Fourier maps, and H positions were refined using the soft constraints that O−H bonds be ∼0.96 Å. The structures were successfully refined by least-squares methods, on the basis of F^2 for all unique data and including anisotropic displacement parameters for all atoms. Refinements for KS2-2 and NaS2-2 converged and gave R_1 values of 0.035 for 4842 unique reflections ($F_o \geq 4\sigma$) and 0.036 for 3376 unique reflections ($F_o \geq 4\sigma$), respectively. The atomic positional parameters and anisotropic displacement parameters are given in the Supporting Information. Tables 2 and 3 contain selected interatomic distances for KS2-2 and NaS2-2, respectively.

Magnetic Measurements. Magnetization measurements were conducted using polycrystalline samples of NaS2-2 and KS2-2, using a superconducting quantum interference device (SQUID) magnetometer, over the temperature range 5−320 K. The radiological hazards associated with ^{237}Np necessitated double encapsulation of the samples in sealed aluminum holders that contributed significantly (approximately 80%) to the measured signals in the worst case. Susceptibility data were obtained from 6.8 mg of NaS2-2 and 1.6 mg of KS2-2 under an applied field of 2000 G. Additional temperature-dependent measurements were conducted at various fields, as low as 20 G, over the range of 5−20 K to examine evidence for long-range magnetic ordering. Variable-field hysteresis measurements were also done over this temperature range to fields as high as 25 000 G. Empty Al sample holders were measured separately under identical conditions, and their magnetic response was subtracted directly from the raw data. The diamagnetic response of the sample was calculated and removed from the data in each case.

Table 3. Bond Lengths [Å] for NaS2-2

Np(1)−O(7)[a]	1.819(4)	Na(2)−O(7)[d]	2.482(5)
Np(1)−O(9)	1.845(4)	Na(2)−O(7)	2.482(5)
Np(1)−O(6)[a]	2.454(4)	Na(2)−O(1)[e]	2.556(5)
Np(1)−O(8)	2.460(5)	Na(2)−O(1)[f]	2.556(5)
Np(1)−O(3)	2.474(4)	Na(2)−O(3)	2.850(5)
Np(1)−O(2)[a]	2.472(4)	Na(2)−O(3)[d]	2.851(5)
Np(1)−O(1)	2.479(4)		
		Na(3)−O(14)	2.294(6)
Np(2)−O(6)	1.838(4)	Na(3)−O(13)[g]	2.306(6)
Np(2)−O(10)	1.851(4)	Na(3)−O(13)	2.340(6)
Np(2)−O(10)[b]	2.418(4)	Na(3)−O(4)[h]	2.376(5)
Np(2)−O(9)	2.431(4)	Na(3)−O(5)[h]	2.395(5)
Np(2)−O(11)	2.452(4)	Na(3)−O(8)	2.934(6)
Np(2)−O(4)	2.486(4)		
Np(2)−O(5)	2.522(5)	S(1)−O(13)	1.458(5)
		S(1)−O(2)[c]	1.478(4)
Na(1)−O(12)	2.389(5)	S(1)−O(8)	1.480(5)
Na(1)−O(12)[c]	2.389(5)	S(1)−O(12)[a]	1.478(5)
Na(1)−O(2)[c]	2.466(4)		
Na(1)−O(2)	2.466(4)	S(2)−O(3)[d]	1.466(4)
Na(1)−O(8)	2.871(5)	S(2)−O(1)	1.470(4)
Na(1)−O(8)[c]	2.871(5)	S(2)−O(4)[i]	1.482(5)
		S(2)−O(11)	1.487(4)
Na(2)−O(11)[d]	2.411(5)		
Na(2)−O(11)	2.411(5)		

[a −i]Symmetry transformations used to generate equivalent atoms: (a) $-x, y, -z + 1/2$; (b) $-x + 1/2, y + 1/2, -z + 1/2$; (c) $-x - 1/2, -y + 3/2, -z$; (d) $x - 1/2, y + 1/2, z$; (e) $-x + 1/2, y - 1/2, -z + 1/2$; (f) $x, y + 1, z$; (g) $x, y - 1, z$; (h) $x + 1/2, y - 1/2, z$; (i) $-x, -y + 1, -z$.

Results

Single-Crystal X-ray Diffraction. The structures of KS2-2 and NaS2-2 are isostructural frameworks of linked neptunyl and sulfate polyhedra. Each structure contains two symmetrically independent Np^{5+} cations, each of which is strongly bonded to two atoms of O_{Np}, forming approximately linear $(NpO_2)^+$ neptunyl ions. The $[O_{Np}{=}Np{=}O_{Np}]^+$ bond lengths range from 1.814 to 1.856 Å, consistent with the pentavalent oxidation state of Np. Each of the neptunyl ions is coordinated by five additional O or H_2O ligands arranged at the equatorial vertexes of pentagonal bipyramids that are capped by dioxo O_{Np} ligands. The structures each also contain two symmetrically distinct sulfate tetrahedra, with average S−O bond lengths ranging from 1.458 to 1.488 Å.

The neptunyl pentagonal bipyramids and sulfate tetrahedra are linked into a complex framework by sharing vertexes. However, the structural connectivity is dominated by ribbons of polyhedra that extend along the [010] direction (Figure 1). Neptunyl bipyramids form the backbone of the ribbon, which is four Np wide and contains both Np(1) and Np(2). The Np(2) bipyramids are located toward the center of the ribbon. Each Np(2) polyhedron is linked to two Np(2) and two Np(1) bipyramids by sharing vertexes. The Np(1) polyhedra, which truncate the ribbons on either side, are each only linked to two Np(2) polyhedra.

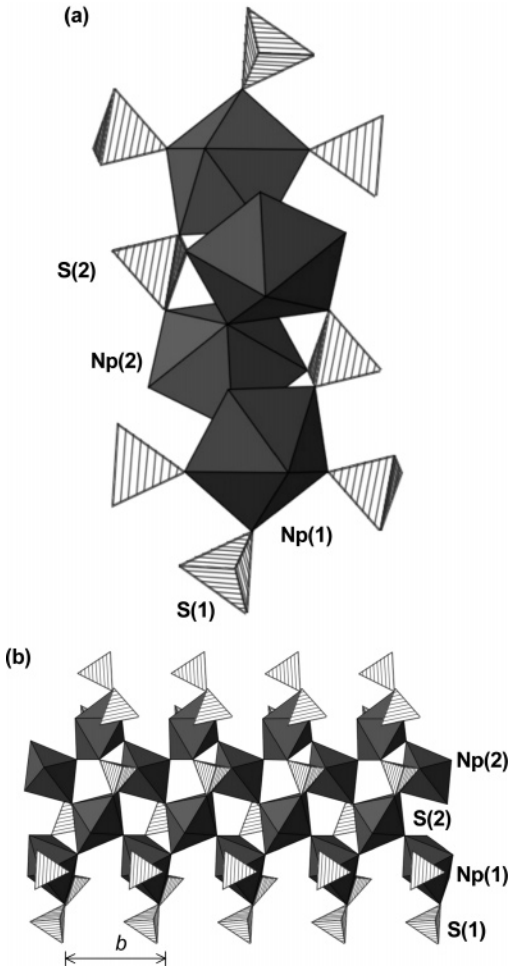

Figure 1. Ribbons of neptunyl pentagonal bipyramids and sulfate tetrahedra (a) that extend along the [010] direction (b) in the structures of $NaK_3(NpO_2)_4(SO_4)_4(H_2O)_2$ and $NaNpO_2SO_4H_2O$.

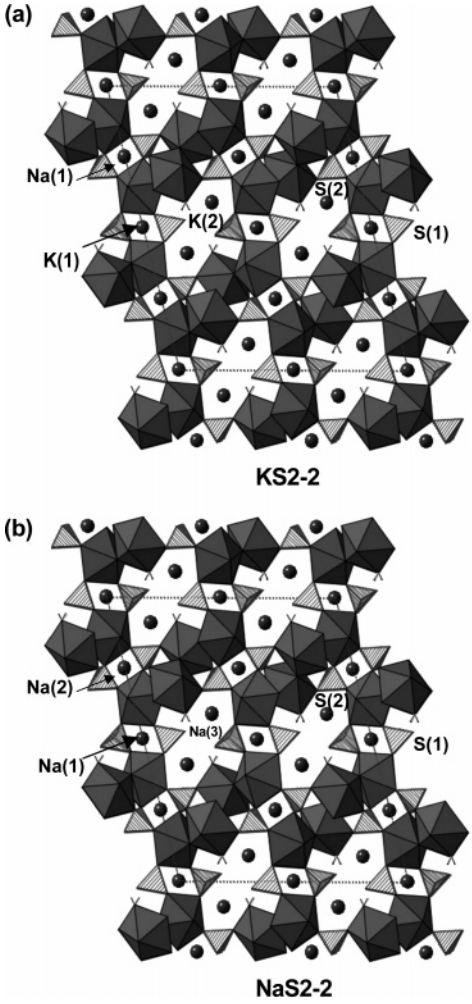

Figure 2. Polymerization of the neptunyl bipyramid ribbons through S(1) and S(2) tetrahedra to create the framework structure observed in $NaK_3(NpO_2)_4(SO_4)_4(H_2O)_2$ (a) and $NaNpO_2SO_4H_2O$ (b). Interstitial voids contain monovalent cations and H_2O groups.

The linkages between the Np polyhedra warrant special consideration, as several cation−cation interactions exist. Both of the O_{Np} atoms bonded to the Np(2) form cation−cation interactions, one with another Np(2) and the other with an adjacent Np(1). Thus, each Np(2) polyhedron includes two equatorial vertexes that are O_{Np} atoms of adjacent polyhedra. Np(1) forms one cation−cation interaction between the O_{Np} atom in the Np(1) polyhedron and the equatorial vertex of Np(2). One equatorial vertex of Np(1) is also the O_{Np} of the adjacent Np(2) polyhedron.

The ribbon of neptunyl pentagonal bipyramids is decorated with two types of sulfate tetrahedra, each of which shares vertexes with the neptunyl polyhedra, as shown in Figure 1b. In all cases where the linkage of a tetrahedron and bipyramid exists, the shared ligand is located in an equatorial position of the bipyramid. Each S(2) tetrahedron is attached on the interior of the ribbon, where it shares two vertexes with Np(2) polyhedra and one with a Np(1) polyhedron. The fourth vertex on the S(2) tetrahedron is bonded to the equatorial oxygen of Np(1) of the adjacent chain, providing a linkage into a framework. Each S(1) tetrahedron shares one vertex with the equatorial oxygen of a Np(1) polyhedron and one with a Np(1) polyhedron of an adjacent chain.

All equatorial oxygen atoms of the Np(1) bipyramid are linked to other polyhedra involving higher-valent cations: four oxygen atoms are shared with sulfate tetrahedra, and the fifth is involved in a cation−cation interaction with a Np(2) polyhedron. Two of the equatorial oxygen atoms of the Np(2) polyhedron are involved in cation−cation interactions, two vertexes are shared with sulfate tetrahedra, and one is a H_2O group.

Remarkably, neptunyl bipyramids do not share equatorial vertexes in the structure of KS2-2 or NaS2-2, except via cation−cation interactions. Additional linkages within the framework are through the sulfate tetrahedra. Equatorial vertexes of the neptunyl polyhedra in adjacent ribbons are linked through SO_4 tetrahedra and by bonds to low-valence cations (Figure 2).

Three types of interstitial voids exist between the neptunyl sulfate ribbons with three symmetrically independent K or Na cations located within these voids (Figure 2). One cation is located between the S(2) tetrahedra, and another is located in the void delineated by the S(1) tetrahedra. As a result of framework linkage, a third, larger void is created that contains the additional cation and water groups.

The two independent K cations in KS2-2 are located between the two S(1) tetrahedra and in the larger void created by linkage into the framework. The K(1) and K(2) cations are bonded to eight and seven oxygen atoms, respectively,

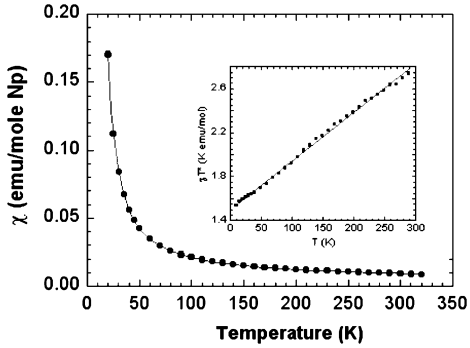

Figure 3. Magnetic susceptibility data obtained from a 6.8 mg sample of NaS2-2 under an applied field of 2000 G. The line through the data represents the best fit for the parameters listed in Table 4. The inset shows the same data plotted as χT^* vs T^*, where $T^* = T - \theta$ and represents the temperature corrected for the experimentally determined Weiss constant. The slope of the data confirms the relatively large magnitude of the temperature-independent contribution to the susceptibility.

with bond lengths ranging from 2.658(4) to 3.227(4) Å. The Na cation is located between the S(2) polyhedra and is coordinated by eight oxygen atoms with an average bond length of 2.571 Å.

In NaS2-2, the Na(1) and Na(3) cations are octahedrally coordinated with bond lengths ranging from 2.294(6) to 2.934(6) Å. The anisotropic displacement parameters for Na(1) are large, consistent with disorder or a split site. Fourier maps of the electron density around Na(1) exhibit elongation along [001] but no splitting of the site. The Na(2) cation is coordinated by eight oxygen atoms with an average bond length of 2.574 Å. A water group is also located within the void bounded by S(2) tetrahedra, where it is held in place by H bonds only. The H bonds in this H_2O group [O(14)] extend to oxygen acceptors on the S(1) tetrahedra [O(12)] and an equatorial vertex of the Np(1) polyhedra [O(7)]. The oxygen acceptor lengths are 1.89 Å for H(1)−O(12) and 2.03 Å for H(3)−O(7).

Both structures also contain a H_2O ligand at one equatorial vertex of the Np(2) polyhedron. For NaS2-2, the H bonds from O(5) extend to the oxygen acceptors on the S(1) tetrahedron O(12) and to the O(14) interstitial H_2O group. The acceptor lengths are 1.78 Å for H(2)−O(7) and 1.98 Å for H(4)−O(12). For KS2-2, the H bonds from O(5) extend to oxygen acceptors on the S(1) tetrahedra [O(12) and O(13)] with bond lengths of 1.93 Å and 1.88 Å, respectively.

Magnetic Properties. The magnetic susceptibility data collected for the NaS2-2 sample, measured under an applied field of 2000 G over the temperature range 20−320 K, are shown in Figure 3. The data are fit to a modified Curie law:

$$\chi_{exp} = \frac{C}{T-\theta} + \chi_{TIP}$$

in which θ, the Weiss constant, is an indication of the interaction energy between local spins, expressed as a temperature, and χ_{TIP} is the temperature-independent paramagnetism (TIP). C is the Curie constant and is related to the effective magnetic moment by

$$\mu_{eff} = \left(\frac{3kC}{N\mu_B^2}\right)^{1/2}$$

Table 4. Fitted Parameters from Magnetic Susceptibility Data As Discussed in the Text[a]

	C (mol K)	θ (K)	χ_{TIP} (emu/mol)	μ_{eff} (μ_B)	T_c (K)	μ_{SAT} (μ_B)
NaS2-2	1.50(1)	11.6(5)	0.0044(1)	3.47(10)	7.4(1)	2.1(2)
KS2-2	1.7(2)	9.9(5)	0.0075(1)	3.65(20)	6.5(5)	2.4(2)
Np^{5+} free ion	1.6			3.58		3.2

[a] The results are reported per mole of Np and are compared with the free ion moment, assuming Russell−Saunders coupling of a f^2 configuration.

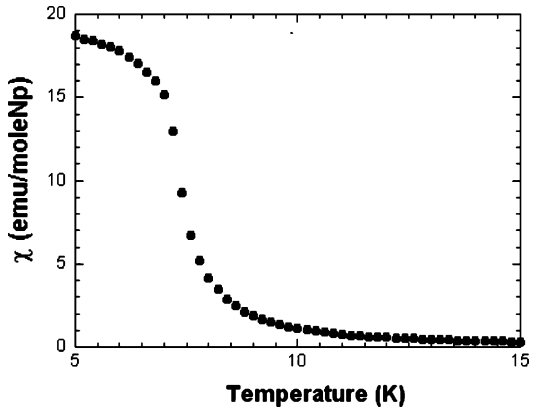

Figure 4. Low-field susceptibility of NaS2-2 measured under an applied field of 20 G. The sharp rise in magnetic response at low temperature is interpreted as the onset of long range ordering of the Np moments, with a T_c of 7.4(1) K.

with k as the Boltzmann constant, N as Avogadro's number, and μ_B as the units of Bohr magnetons, equal to 0.927×10^{-20} erg/Gauss. The best fits to the data are listed in Table 4. The effective moments, calculated from the Curie constants, are within 5% of the free-ion effective moment of $\mu_{eff} = 3.58\ \mu_B$ expected for an f^2 system using the Russell−Saunders coupling scheme. The rather large values of the TIP contributions, confirmed by a plot of χT versus T as shown in the inset of Figure 3, are consistent with those previously observed in other actinide oxides[15] and within the range expected for a molecular crystal in which the major contribution would arise from second-order crystal-field effects (vanVleck paramagnetism). The Weiss constant is small and positive, indicating either ferromagnetic spin interactions and/or crystal-field effects.[16]

The low-temperature susceptibility, obtained from the same NaS2-2 sample in an applied field of 20 G, is shown in Figure 4. The data indicate a spontaneous magnetic ordering of the Np moments at 7.4(1) K. The field response of the magnetization at 5 K, shown in Figure 5, exhibits saturation behavior at low field, consistent with a ferromagnetic coupling of the moments. The saturation value of the magnetization, μ_{SAT}, representing the high field limit of the magnetization, is related to the electronic ground state according to

$$\mu_{SAT} = -gJ\mu_B$$

where J represents the total angular momentum in the

(15) Bickel, M.; Kanellakopulos, B. *J. Solid State Chem.* **1993**, *107*, 273−284.
(16) Ziman, J. M. *Principles of the Theory of Solids*; Cambridge University Press: Cambridge, 1979; p 435.

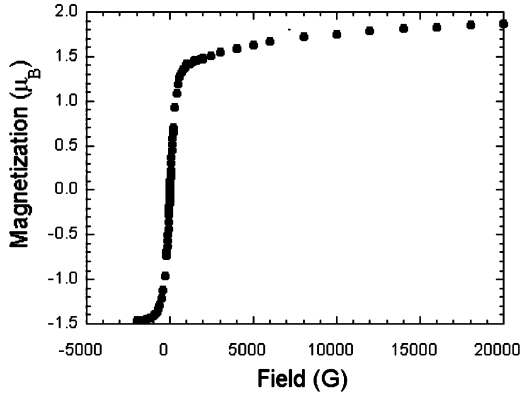

Figure 5. Field dependence of the NaS2-2 magnetization at 5 K, below the ordering temperature. An extrapolation of these data to high field is used to determine the Np saturation moment.

Russell−Saunders formalism. The experimentally determined magnetization extrapolates to 2.1(2) μ_B for NaS2-2 and 2.4(2) for KS2-2, which are significantly less than the 3.2 μ_B expected for a full-moment f^2 system. Crystal-field splitting could reduce the moment observed here[17,18] because the strong axial symmetry felt by the Np ion in the neptunyl unit reduces the free-ion spherical symmetry. This effect requires the replacement of J states with wave functions Γ_n that include the appropriate mixing of $|m_J\rangle$ states. Crystal-field effects have been previously shown to account for similar reductions in the Pr^{3+} saturation moments in oxide systems. Pr^{3+}, which also has an f^2 configuration, has reported saturation moments ranging from negligible to about 2 μ_B or larger.[18,19] It should be noted that the attribution of a single saturation moment for Np based upon magnetization data from a powder sample may be problematic in this case because there are two crystallographically inequivalent neptunyl moieties in the structure, with their principal axes aligned in perpendicular directions. Although such a geometry could affect the averaging of crystal-field states, the ease of saturation exhibited in the field-dependent magnetization curve suggests that orientation effects do not play a dominant role in the moment reduction. An alternate but related explanation for the reduced saturation could arise if the ordering involves a canted-spin orientation that partially cancels the observed moment. Further single-crystal studies are required to sort out these ambiguities.

Discussion

U^{6+}, Np^{5+}, and Np^{6+} in solutions and the solid state form dioxo cations surrounded by oxygen atoms or H_2O groups. In solution the uranyl(VI), neptunyl(VI), and neptunyl(V) ions have An═O bond lengths of 1.77(1), 1.73(2), and 1.80(2) Å, respectively.[5,20] The dioxo cations are equatorially coordinated by H_2O groups with bond lengths of 2.41(8), 2.44(3), and 2.36(3) Å for U^{6+}, Np^{5+}, and Np^{6+}, respectively.[5,20] In solution Np^{6+} tends to have shorter bonds than Np^{5+}, and the same trend is also present in the solid state. In $Cs_2Np(VI)O_2(SO_4)_2$, the bond lengths for Np^{6+} are 1.75(1) Å for the neptunyl ion and 2.37(19) Å for equatorial coordination.[21] The average bond lengths for the reported Np^{5+} sulfates are 1.83(1) Å for the dioxo ion and 2.48(6) Å for the equatorial distances.[22−25] KS2-2 and NaS2-2 display average bond lengths of 1.84(1) Å for the neptunyl ion and 2.46(1) Å for the equatorial ligands, which is consistent with the pentavalent state of neptunium.

In the structure of KS2-2, one Na cation is found in the interstitial void between the two S(2) tetrahedra. Sodium was not added to the synthesis but is thought to be a contaminant introduced during the purification of the $(NpO_2)^+$ stock solution. After passing a $(NpO_2)^+$ solution through an ion-exchange column, a concentrated NaOH solution is used to precipitate a Np^{5+} hydroxide. The solid is washed several times with water and then redissolved in the appropriate amount of 1 M HCl to create the 0.100 M $(NpO_2)^+$ stock solution. Excess NaOH causes a sodium neptunyl hydroxide solid to precipitate, and sodium can become a contaminant in the stock solution.

Fifteen uranyl sulfate minerals have been described from nature, and their structures are dominated by polymerization of uranyl polyhedra and sulfate tetrahedra to form chains and sheets.[26,27] In minerals, the linkages between sulfate tetrahedra and uranyl polyhedra are limited to vertex sharing, and no cation−cation interactions are present. In contrast, the neptunyl sulfates KS2-2 and NaS2-2 are frameworks of polyhedra, and the only direct linkages between neptunyl polyhedra are through cation−cation interactions, as demonstrated in Figures 1 and 2.

The structure of $Cs_3NpO_2(SO_4)_2(H_2O)_2$ has infinite chains of edge-sharing neptunyl pentagonal bipyramids and does not have cation−cation interactions.[23] Several neptunyl sulfates with composition $(NpO_2)_2SO_4(H_2O)_x$ have been reported, and the structures of $(NpO_2)_2SO_4H_2O$ and $(NpO_2)_2SO_4(H_2O)_2$ have been described.[22,24,28] The structure of $(NpO_2)_2SO_4H_2O$ consists of a framework of neptunyl pentagonal bipyramids, distorted neptunyl hexagonal bipyramids, and sulfate tetrahedra. Each Np^{5+} cation is involved in four cation−cation interactions, with each O_{Np} also acting as the equatorial oxygen of the neighboring polyhedra.[24] The

(17) Wybourne, B. G. *Spectroscopic Properties of Rare Earths*; Interscience: New York, 1965; p 236.
(18) Staub, U.; Soderholm, L. In *Handbook on the Physics and Chemistry of Rare Earths*; Schneidner, K. J., Eyring, L., Maple, M. B., Eds.; Elsevier Science: New York, 2000; Vol. 30, pp 491−545.
(19) Lea, K. R.; Leask, J. M.; Wolf, W. P. *J. Phys. Chem. Solids* **1962**, 23, 1381−1405.
(20) Moll, H.; Reich, T.; Hennig, C.; Rossberg, A.; Szabo, Z.; Grenthe, I. *Radiochim. Acta* **2000**, *88*, 559−566.
(21) Fedosseev, A. M.; Budantseva, N. A.; Grigoriev, M. S.; Bessonov, A. A.; Astafurova, L. N.; Lapitskaya, T. S.; Krupa, J.-C. *Radiochim. Acta* **1999**, *86*, 17−22.
(22) Grigor'ev, M. S.; Yanovskii, A. I.; Fedoseev, A. M.; Budantseva, N. A.; Struchkov, Y. T.; Krot, N. N.; Spitsyn, V. I. *Dokl. Akad. Nauk SSSR* **1988**, *300*, 618−622.
(23) Grigor'ev, M. S.; Yanovskii, A. I.; Fedoseev, A. M.; Budantseva, N. A.; Struchkov, Y. T.; Krot, N. N. *Radiokhimiya* **1991**, *33*, 17−19.
(24) Grigor'ev, M. S.; Baturin, N. A.; Budantseva, N. A.; Fedoseev, A. M. *Radiokhimiya* **1993**, *35*, 29.
(25) Forbes, T. Z.; Burns, P. C. *J. Solid State Chem.* **2005**, *178*, 3445−3452.
(26) Burns, P. C. *The Crystal Chemistry of Uranium*; Mineralogical Society of America: Washington, DC, 1999.
(27) Burns, P. C.; Deely, K. M.; Hayden, L. A. *Can. Mineral.* **2003**, *41*, 687−706.
(28) Budantseva, N. A.; Fedoseev, A. M.; Grigor'ev, M. S.; Potemkina, T. I.; Afanas'eva, T. V.; Krot, N. N. *Radiokhimiya* **1988**, *30*, 607−610.

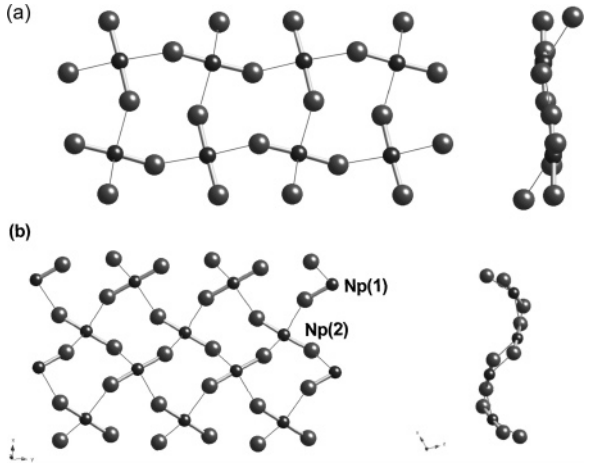

Figure 6. Cation−cation interactions found in $(NpO_2)_2(NO_3)_2(H_2O)_5$. Part (a) exhibits three cation−cation interactions creating the nearly linear neptunyl polyhedra ribbon.[24,25] The ribbon found in KS2-2 and NaS2-2 (b) has two types of neptunyl polyhedra with Np(1) involved in two cation−cation interactions and Np(2) involved in four cation−cation interactions.

structure of $(NpO_2)_2SO_4(H_2O)_2$ has two symmetrically independent neptunyl pentagonal bipyramids, and the neptunyl ions participate in four cation−cation interactions that lead to the formation of an infinite sheet of neptunyl polyhedra.[22]

The ribbons of neptunyl polyhedra in KS2-2 and NaS2-2 may be compared to those in the structures of $NpO_2ClO_4(H_2O)_4$ and $(NpO_2)_2(NO_3)_2(H_2O)_5$. $NpO_2ClO_4(H_2O)_4$ has neptunyl polyhedra linked by cation−cation interactions into a zigzag chain with the linear neptunyl ion oriented approximately perpendicular to the adjacent neptunyl ion.[11,29] The cation−cation interactions in $(NpO_2)_2(NO_3)_2(H_2O)_5$ give ribbonlike chains of neptunyl polyhedra, and the neptunyl ions are each involved in three cation−cation interactions as shown in Figure 6.[11,30] This structure has both neptunyl pentagonal bipyramids and hexagonal bipyramids. They are linked, creating chains extending in the [010] direction, and the nearly linear ribbons of neptunyl pentagonal bipyramids are two Np polyhedra wide, as shown in Figure 6a.

The structures of KS2-2 and NaS2-2 exhibit ribbons that are four neptunyl polyhedra wide and include a different number of cation−cation interactions for the two independent neptunyl ions. Np(1) forms two cation−cation interactions whereas Np(2) forms four by linking to two Np(1) polyhedra and two neighboring Np(2) polyhedra. The chain of neptunyl pentagonal bipyramids is curved in the third dimension to accommodate these linkages (Figure 6b). The cation−cation interactions result in distinctive ribbons of neptunyl polyhedra.

Despite the relative rarity of ferromagnetic ordering in molecular, nonconducting systems, the apparent ferromagnetism observed for both NaS2-2 and KS2-2 is not without precedent. For example, ferromagnetism is observed in $NpO_2(O_2CH)(H_2O)$ below 12.3 K[31] and in β-$AgNpO_2SeO_3$[32] below about 8 K. $(NpO_2)_2(O_2C)_2C_6H_4(H_2O)_3H_2O$ exhibits complex behavior consistent with a ferromagnetic Np^{5+} sublattice below 4.5 K and a metamagnetic Np^{5+} sublattice at higher fields.[33] Evidence of magnetic ordering is also present in $Na_4(NpO_2)_2C_{12}O_{12}(H_2O)_8$ at 10 K[34] although the nature of the ordering is unclear. In addition to magnetic ordering at temperatures of about 10 K, these compounds share a common structural feature: They all exhibit cation−cation interactions.[9] The result is a Np−Np distance of about 4.1 Å, connected via a bridging oxygen. This metal linkage can result in chains or planar networks of closely associated Np ions. Such linkages provide superexchange pathways that may serve to enhance magnetic interactions and thus affect magnetic ordering. The diversity seen in Np(V) structures exhibiting cation−cation interactions may serve as a tool to study superexchange pathways and their influences on magnetic ordering of *f*-ion spins.

Acknowledgment. This research was supported by the National Science Foundation Environmental Molecular Science Institute at the University of Notre Dame (EAR02-21966). The work at Argonne National Laboratory was supported by the U.S. DOE−BES, Chemical Sciences, under Contract No. W-31-109-ENG-38.

Supporting Information Available: X-ray crystallographic information files (CIF), atomic coordinates, and equivalent isotropic displacement parameters (PDF) for KS2-2 and NaS2-2. This material is available free of charge via the Internet at http://pubs.acs.org.

CM0523687

(29) Grigor'ev, M. S.; Baturin, N. A.; Bessonov, A. A.; Krot, N. N. *Radiokhimiya* **1995**, *37*, 15−18.
(30) Grigor'ev, M. S.; Charushnikova, I. A.; Krot, N. N.; Yanovskii, A. I.; Struchkov, Y. T. *Zh. Neorg. Khim.* **1994**, *39*, 179−183.
(31) Nakamoto, T.; Nakada, M.; Nakamura, A.; Haga, H.; Onuki, Y. *Solid State Commun.* **1999**, *109*, 77−81.
(32) Jobiliong, E.; Oshima, Y.; Brooks, J. S.; Albrecht-Schmitt, T. E. *Solid State Commun.* **2004**, *132*, 337−342.
(33) Nakamoto, T.; Nakada, M.; Nakamura, A. *J. Nucl. Sci. Technol.* **2002** (Suppl. 3), 102−105.
(34) Nectoux, F.; Abazli, H.; Jove, J.; Cousson, A.; Pages, M.; Gasperin, M.; Choppin, G. *J. Less-Common Met.* **1884**, *97*, 1−10.